

Received 4 December 2024, accepted 18 December 2024, date of publication 26 December 2024, date of current version 2 January 2024.

Digital Object Identifier 10.1109/ACCESS.2024.3 2341



Transmission Failure Prediction Using AI and Structural Modeling Informed by Distribution Outages

^{ID}, (Member,),

^{ID}3,4,

^{ID}1,

Corresponding author: ()

This work was supported in part by (), and in part by

ABSTRACT Understanding and quantifying the impact of severe weather events on the electric transmission and distribution system is crucial for ensuring its resilience in the context of the increasing frequency and intensity of extreme weather events caused by climate change. While weather impact models for the distribution system have been widely developed during the past decade, transmission system impact models lagged behind because of the scarcity of data. This study demonstrates a weather impact model for predicting the probability of failure of transmission lines. It builds upon a recently developed model and focuses on reducing model bias, through multi-model integration, feature engineering, and the development of a storm index that leverages distribution system data to aid the prediction of transmission risk. We explored three methods for integrating machine learning with mechanistic models. They consist of: (a) creating a linear combination of the outputs of the two modeling approaches, (b) including fragility curves as additional inputs to machine learning models, and (c) developing a new machine learning model that uses the outputs of the weather-based machine learning model, fragility curve estimates, and wind data to make new predictions. Moreover, due to the limited number of historical failures in transmission networks, a storm index was developed leveraging a dataset of distribution outages to learn about storm behavior to improve model skills. In the current version of the model, we substantially reduced the overestimation in the sum of predicted values of transmission line probability of failure that was present in the previously published model by a factor of 10. This has led to a reduction of model bias from 33.2% to 14.46–1.43%. The model with the integrated approach and storm index demonstrates substantial improvements in the estimation of the probability of failure of transmission lines and their ranking by risk level. The improved model is able to capture 60% of the failures within the top 22.2% of the ranked power lines, compared to a value of 34.9% for the previous model. With an estimate of the probability of failure of transmission lines ahead of storms, power system planning and maintenance engineers will have critical information to make informed decisions, to create better mitigation plans and minimize power disruptions. Long term, this model can assist with resilience investments as it highlights areas of the system more susceptible to damage.

The associate editor coordinating the review of this manuscript and approving it for publication was Mouquan Shen ^{ID}.

INDEX TERMS Failure prediction, machine learning, transmission system, structural modeling.

I. INTRODUCTION

Each component of the power system—generation, transmission, and distribution - exhibits varying levels of vulnerability to environmental challenges from climate change [1], [2], [3], [4], [5], [6], [7], [8], [9]. Heightened frequency and intensity of weather events erode confidence in load loss predictions [10]. Increased weather event frequency and intensity also impact reliability and resilience. Hotter summers drive increased air conditioning usage, elevating utility loads [11]. Extreme weather variability strains generation structures, exacerbating wear and tear [12]. Traditionally, generation vulnerabilities focused on cyberattacks, but the addition of renewables to the grid introduces new risks, namely power generation reliability [13], [14], [15], [16]. Weather-dependent renewables rely on accurate forecasts to manage load losses, with extreme events dictating offline decisions to prevent damage [17]. Substations, often in flood-prone, remote areas, face heightened risk from wetter weather, necessitating shutdowns to mitigate harm to humans and equipment [10]. Transmission networks, despite continuous maintenance, experience increasing failures during severe weather. Prolonged, strong winds transport debris, potentially compromising structural integrity and prompting load removal to prevent further damage [18]. Distribution systems, characterized by overhead wires vulnerable to human and environmental factors, suffer even more frequent damage, hindering utility service coverage [19].

To address these emerging vulnerabilities, data-driven models have been increasingly used to optimize power generation [20], [21], [22], calculate electricity load [23], [24], predict potential failures and uncertainties [25], [26], [27], and optimize electric power management [28], [29], [30]. Some of these models also utilize an integrated ML approach to reach optimal results [31]. These models leverage historical data, weather forecasts, and real-time sensor inputs to simulate various stress scenarios, helping utilities proactively manage risks and maintain reliability even in the face of extreme weather events and the growing integration of renewable energy sources.

Given the increasing risks posed by extreme weather events and the integration of weather-dependent renewable energy, the distribution network is particularly vulnerable to environmental factors. During severe weather events, energy resiliency and reliability issues are commonly associated with the distribution network. However, transmission systems also face significant challenges. While failures in transmission networks occur less frequently than in distribution systems, they have a larger impact, affecting more customers and causing greater economic losses per incident. Despite numerous studies on distribution network failures, which have primarily investigated the environmental impacts on power generation [32], [33], [34], [35], [36], [37], [38], [39], [40], [41], [42], [43], [44], [45], [46], [47], [48], [49], restoration

time factors [50], and other reliability issues [51], [52], [53], [54], [55], research specifically addressing causes associated with transmission network weather-related failures is limited.

In transmission networks, studies have explored risk mitigation strategies related to environmental factors. Early work utilized statistical models to analyze transmission line designs prone to failures [1], [56], [57], [58], while recent research has investigated the relationship between environmental factors and transmission lines [59]. Advanced methods now integrate weather data into predictive models [60], [61], [62], [63], [64], [65], [66].

Two recent papers, integrating concepts developed in the University of Connecticut Outage Prediction Model (UConn OPM), [65], [66] explore the use of machine learning techniques for understanding risk in the transmission system. Reference [65] focused on expanding the literature on understanding the factors that contribute to failures within the transmission system. A machine learning prototype that leverages historical failure, infrastructure, and environmental data was created to predict the risk imposed on each transmission line within the Eversource Energy territories. Using this prototype called the Failure Prediction Model (FPM), the model was able to provide ranked risk forecasts for transmission lines more susceptible to failures. Additionally, [66] explored the combination of a physics-based and data-driven approach to understand failure risk within the transmission system. A machine learning model leverages the physics-based model's ability to understand wind-dependent failures while the data-driven approach accounts for wind-independent failures. This framework was tested on overhead transmission systems in the Eversource Energy territories which showed improved predictions of storm failures.

We aim to bridge the gap in transmission failure data availability and understanding by leveraging knowledge from distribution systems for a comprehensive study on transmission networks. This study integrates concepts developed in the UConn OPM, an outage prediction model used to predict distribution outages due to environmental impacts [33], [36], [39], [43], [67], and FPM, a combined physics and machine learning-based model, used to forecast failure risk in transmission system [65], [66]. These transmission and distribution studies underscore the effectiveness of integrating climate, land use, weather, and infrastructure data to understand and predict the impact of extreme weather. Understanding factors contributing to outages will be leveraged as a foundational framework to forecast transmission system failures.

This research focuses on three main objectives. The first is reducing bias in the transmission failure risk prediction model by employing refined variable selection and utilizing hyperparameter tuning. The second is creating and assessing three methods for integrating mechanistic and machine learning models: (a) developing linear combinations of multiple model

outputs, (b) implementing mechanistic model outputs into machine learning training, and (c) constructing a two-step model that combines the predictions of machine learning and mechanistic models previously computed with wind variables. The third is developing and utilizing a storm index that capitalizes on the higher availability of data in the distribution system to predict risks within the transmission system by leveraging failure correlation between the two systems. Section II outlines the methodology, starting with the FPM framework (2.A), leveraging diverse datasets for enhanced feature input (2.B), employing various machine learning approaches (2.C), integrating mechanistic model outputs (2.D), leveraging distribution outage prediction outputs (2.E) and evaluation metrics to understand model performance (2.F). Section III presents results: machine learning (3.A), the integrated model (3.B), and the storm index addition (3.C). Section IV looks at a case study of the top storm to cause the most sustained failures. Section V concludes with findings, discussion, and limitations. Section V provides the final list of variables used in the machine learning model.

II. METHODOLOGY

A. FPM ARCHITECTURE

The framework of the FPM consists of combining weather, land cover, vegetation, infrastructure, and historical failure data (Figure 1). The data used was extracted from multiple sources and refined using different algorithms and domain knowledge. These data include weather, tree height, tree type, pole structure types, transmission line length, leaf area index, and failure data. Fragility curve and storm index information were also added to the machine learning inputs to leverage their information to enhance the machine learning predictions. Multiple machine learning models were used with different parameters to identify the model with the best accuracy score. The best model was then optimized using hyperparameter tuning. The results from the model are then cross-validated before predicting transmission risk.

B. INPUT DATA

The weather data used was extracted using the Weather Research and Forecasting Model (WRF) version 3.8.1 model, an advanced research numerical weather prediction model (NWP) [68], [69], used to generate data at 4-km horizontal grid spacing with North American Model (NAM) initial and boundary conditions. Weather data extracted were related to temperature, specific humidity, precipitation, wind, wind gust, and soil moisture conditions. For each weather variable, the mean and maximum temporal values for each storm were first extracted. The spatial mean and maximum along each transmission line was then calculated and are denoted by the prefix “mean_” and “max_” respectively. Similar to [65], land cover data was extracted from the Multi-Resolution Land Characteristics Consortium (MRLC) NLCD at 30-meter resolution [70]. NLCD land cover categories were combined into three new categories to create newer reduced land cover variables as follows:

- LC_Developed: Summation of categories 21 (Developed, Open Space), 22 (Developed, Low Intensity), 23 (Developed, Medium Intensity), and 24 (Developed, High Intensity).
- LC_Wetland: Summation of categories 11 (Open Water), 90 (Woody Wetlands), and 95 (Emergent Herbaceous Wetlands).
- LC_Low/no vegetation: Summation of categories 31 (Barren Land), 71 (Grassland/Herbaceous), 81 (Pasture/Hay), and 82 (Cultivated Crops).

Vegetation data used consists of tree type, tree height and leaf area index (LAI). Tree type data were derived for individual tree species from the National Insect and Disease Risk Map (NIDRM) provided by the United States Forest Services [71]. The two main tree types identified were hardwood and softwood. The average percentage of these tree types in grid cells within a 30-meter buffer around transmission lines was calculated. The tree height value for each line was created by integrating GEDI with Landsat analysis-ready data [72]. The tree height value for each line was calculated by finding the weighted average of all the mean and max of tree height values intersecting each transmission line’s buffer. This weighted average was based on the percentage of the of each tree height found in the given interest area. LAI data was originally extracted from Moderate Resolution Imaging Spectroradiometer (MODIS) [73] and modified by computing its value for each raster grid for an 8-day period throughout the year [67]. An average LAI value is associated with each transmission line segment where the buffer created around the transmission lines intersect with the LAI grid cells.

Topography data, primarily elevation, were obtained from the ASTER Global Digital Elevation Model (GDEM) Version 3 (ASTGTM) [74] at a spatial resolution of 1 arc second. A 30-meter buffer around the transmission lines was used to compute the mean, maximum, and standard deviation of elevation at the intersections with the raster.

Infrastructure data was provided by Eversource Energy. This data consisted of shapefiles of transmission lines, structure type, and age of structures. Using line names, the transmission lines were aggregated to get the true span of the lines. This resulted in a total of 321 unique transmission lines. Three main voltage levels were identified for the transmission lines: eleven 69-kV, two hundred sixty-five 115-kV and forty-five 345-kV. After discussions with Eversource Energy engineers and some analysis, seven main structure types were identified: single circuit H-Frame (SCHF), double circuit H-Frame (DCHF), single circuit steel pole H-Frame (SCSPHF), single circuit steel pole (SCSP), double circuit steel pole (DCSP), single circuit lattice tower (SCLT), and double circuit laminated wood pole (DCLWP). Unidentified structures were classified as “Other” in the dataset. The age of structures was calculated by using the oldest and youngest dates of construction and the average of all structures along the circuit that made up the transmission lines.

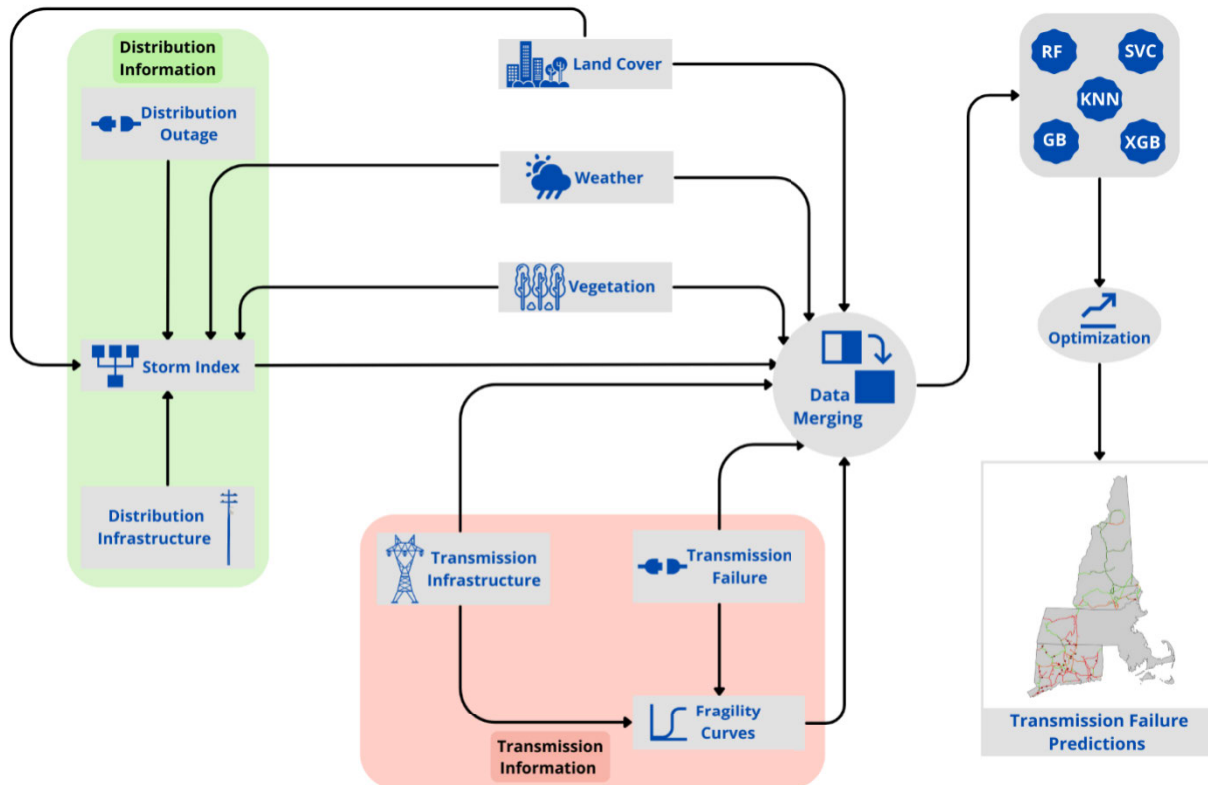


FIGURE 1. FPM framework.

Using the infrastructure data obtained from Eversource Energy, fragility curves were calculated based on physics-based structural models' response under wind forces, using Monte Carlo simulations and finite element modeling. The knowledge of the varied materials and voltages of the seven identified structure types in the transmission system were also used in this calculation. For example, steel towers were observed to be less fragile than wood towers due to their greater stiffness. These fragility curves express the probability of structural failure as a function of a demand parameter, such as wind speed, ice thickness, or dynamic load caused by tree impact on the transmission structures.

A storm index was developed to leverage the larger number of outages available in the Eversource Energy distribution system severe storm dataset to provide storm intensity guidance, to the transmission model. This was possible because the factors contributing to failures are similar in transmission and distribution systems: they consist in the interaction between atmospheric phenomena with vegetation and power lines and manifest as broken branches and uprooted trees falling on power lines [75]. The use of the storm index is to target the limitations of the transmission failure dataset, specifically the under-representation of failures and limited dataset size. The storm index system allows for better understanding of numerical weather prediction outputs and storm strength in the FPM.

The historical failure data from May 2015 to Dec. 2020 was provided by Eversource Energy for a total of 44 storms. The failure data is matched with each transmission line for each of the 44 storms. For lines without failure during a storm, a zero is recorded. This amounts to a total of 14,124 rows of data as there are 44 storms and 321 transmission lines in total. Within these rows, there were 111 failures that were sustained for more than 0 minutes. Overall, the historical failure data used is highly zero-inflated. More information related to the sources of these datasets and the details on how they were synthesized can be found in [65].

C. ML MODELING APPROACH

Consistency in data processing is crucial before modeling to enhance prediction accuracy. Figure 2 shows the modeling approach used once all data was successfully merged. In this modeling method, cross-validation is used, where part of the data is used for training to predict the parts withheld from training. Different machine learning models are then used to identify the best one. Feature importance is applied, in addition to domain knowledge, to perform variable selection. Once variables are selected, this information is used to reduce the dataset, and the process is repeated until the importance threshold is achieved. Hyperparameter tuning is performed to optimize the model's predictions before creating transmission failure predictions.

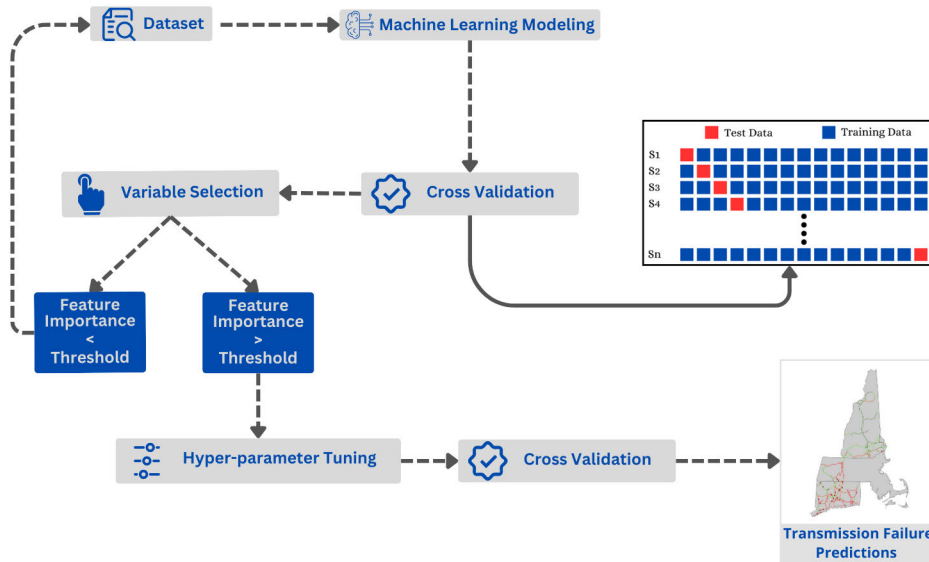


FIGURE 2. Modeling flowchart.

1) ML MODELING

The five models used for the creation of the FPM were Support Vector Machines (SVM), k-Nearest Neighbors (kNN), Random Forest (RF), Gradient Boosting (GB), and Extreme Gradient Boosting (XGB). SVM uses a set of supervised learning algorithms that can be used for classification, regression, and outlier detection [76]. kNN is an algorithm that assumes similar data points are within the same proximity [77]. RF is a supervised learning algorithm that is made up of decision tree algorithms used to solve regression and classification problems [78]. GB is an algorithm made up of an ensemble of weak decision tree models used for regression and classifications [79]. XGB is an algorithm made up of decision trees in a sequential form with weights assigned to each independent variable [80].

Each of these models was trained with the default parameters of their respective python packages. SVM, RF and XGB used the addition of class weighting set to “balanced” when training as this follows the same principles as the balanced scoring metric. XGB was the best model out of the five tested. To optimize model prediction capabilities, variable selection, cross validation and hyper-parameter tuning, were used.

To understand the algorithmic complexity of the proposed method, a comparison is made between the complexity of the proposed method and existing models in supervised learning, including Decision Trees, Random Forests, Gradient Boosting Machines, and Extreme Gradient Boosting. These models differ significantly in their computational demands, training time, memory usage, and overall complexity. Decision Trees (DT) are the simplest, as they recursively split data based on feature values, resulting in a tree structure. While DT are easy to implement and interpret, they can be computationally

inefficient and prone to overfitting if not properly pruned. Random Forests (RF) improve upon DT by aggregating predictions from multiple trees trained on bootstrapped subsets of the data. This ensemble approach increases both model robustness and training time, but it still remains relatively straightforward in terms of complexity, though less interpretable. Gradient Boosting Machines (GBM) add another layer of complexity by building trees sequentially, where each tree corrects the errors of its predecessor. This sequential learning process generally leads to higher accuracy, but at the cost of significantly increased training time and computational resources. Extreme Gradient Boosting (XGB) optimizes GBM by introducing parallelized computation, regularization, and efficient tree-building techniques to reduce both training time and memory usage. XGB is particularly well-suited for large datasets, offering a good balance between performance and efficiency.

In comparison to these existing methods, the proposed model, based on XGB, maintains relatively low computational overhead with very fast training and prediction times. The addition of the fragility curves and the storm index variables does increase computation time slightly, but the overall increase is minimal, suggesting that the proposed method is computationally efficient while retaining the accuracy benefits of XGB. Thus, the proposed method offers a favorable trade-off between model complexity and computational efficiency compared to other popular supervised learning models.

2) CROSS VALIDATION

Cross-validation is a critical component in assessing the performance and robustness of machine learning models. In this study, leave-one-out cross-validation (LOOCV) [81],

[82], [83], a type of k-fold validation, was employed to thoroughly evaluate model capabilities by providing insights into its feasibility. For this process, one storm was excluded from training, and the model's performance was tested on this excluded storm. This process was repeated for each storm in the dataset, resulting in a total of 44 training and testing cycles, corresponding to the 44 storms in the study. LOOCV reduces the degrees of freedom during model evaluation. By leaving out one observation at a time, the model is trained on a slightly smaller-than-full dataset for each iteration, thereby minimizing the risk of information leakage during training and improving its ability to generalize to unseen data.

3) VARIABLE SELECTION

The variables used in machine learning models can have a direct impact on performance. Having multiple correlated variables can contribute to increased noise. To remove some of these correlations, variable selection was performed using domain and environmental knowledge, along with machine learning feature importance. Feature importance in machine learning is a method used to rank the usefulness of data variables as input features in the model to predict the target variable [78], [84]. It is calculated based on the number of times one decision tree's split points improve the model's predictions. Variables with a high feature importance score contribute the most to the model when making predictions [84]. This method allows for the optimal selection of variables used for model training. For the first iteration of the machine learning model training, all variables were used. Each iteration following the first involved some form of variable reduction which showed improvements in model performance. All variables with a feature importance score of less than 0 were eliminated from the input features. After each variable was removed based on feature importance, the model was rerun to assess whether any other variables fell below the threshold for removal. This process continued until no additional variables were identified for elimination. The final iteration of the model included a total of 19 variables, as shown in Appendix in Section V.

4) HYPERPARAMETER TUNING

Hyperparameter tuning is an important step in enhancing the performance and generalizability of machine learning models [85], [86]. While default hyperparameters often provide reasonable results, fine-tuning these parameters can lead to improved model performance. For simplicity, grid search [87] was used to identify the optimal combination of pre-selected hyperparameters to achieve better model accuracy, robustness, and generalization. Grid search works by creating a grid or matrix of different values for each hyper-parameter of interest. The algorithm then systematically explores all possible combinations of these hyperparameter values. For each combination, the model is trained and evaluated, and the best-performing set of hyperparameters is selected. By systematically exploring

various hyperparameter combinations, this approach ensures that the chosen model configuration is well-suited to the specific characteristics of the data, ultimately improving its predictive capabilities.

D. INTEGRATED MODELING APPROACH

In [65] and [66], the capabilities of a machine learning and mechanistic modeling approach are shown respectively for predicting failures in the transmission system. The integration of both modeling approaches is explored to leverage their strengths and understand how this combination improves model predictions. Figure 3 shows the different methods for integration tried and tested.

1) FRAGILITY CURVE

Fragility curves represent the probability of failure of transmission structures for different levels of forcing parameters (Figure 4). In this study, curves that quantify the average number of expected failures in the transmission system caused by the impact of trees forced by wind gusts, or by the direct impact of winds were used. The complex and computationally demanding process of simulating probabilities of damage from tree-induced failures is simplified through parameterization. Parameterized equations are developed based on key variables that effectively predict the failures. For example, the number of equivalent 10-inch diameter trees within range of striking the power line, is selected for its high predictive ability. For more information on the fragility curve calculations, please refer to [66].

2) INTEGRATED MODEL

This integrated model used machine learning model outputs and fragility curve numbers. Fragility curves are calculated using the wind gust, structure age, structure type, and span length and summing each structure's fragility in series to arrive at the circuit-level fragility. The machine learning model outputs are values that range from 0 to 1 to quantify lines more prone to failures. The first approach was a linear model that takes the outputs of the best machine learning model (O_M) and the fragility curves of the transmission lines (O_F). Through a linear combination, it sums a certain percentage of machine learning predictions and a percentage of fragility curve number to create a new prediction for each of the transmission lines. A threshold based on a specific wind speed is set to observe the best combinations for using the machine learning and fragility curve outputs below and above this wind speed value. The second approach takes the fragility curves of the transmission lines as an additional column (O_F) in the dataset (I_M) passed to the machine learning model. In other words, the fragility curve of each transmission line is treated as an additional input to a machine learning model to predict failure risk. The same variable selection for the original model discussed in Section II.C.3 was applied to this model, with the addition of the fragility curve values. The third model takes the fragility curve numbers (O_F), the output of the original machine learning model (O_M) and a

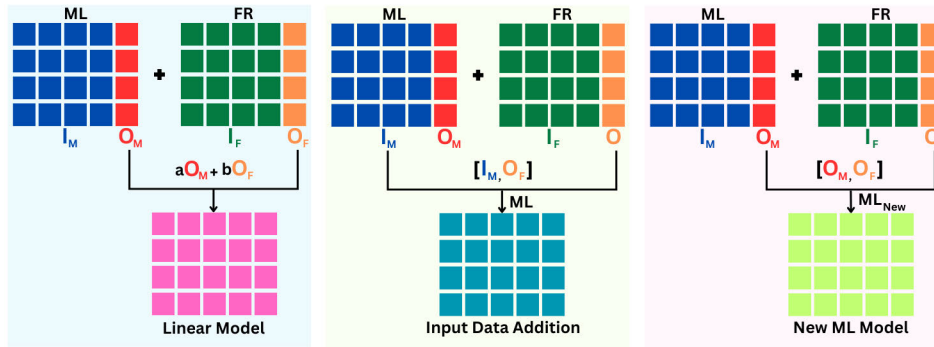


FIGURE 3. Integrated Method Approaches. A) Linear, B) Input data addition and C) New ML model with ML outputs and fragility curve numbers.

wind variable as input in a new machine learning model. The second modeling approach was identified to best-integrated approach to improve model predictions.

E. STORM INDEX

A new model, leveraging storm impacts on distribution systems, was created and calibrated on the Eversource Energy strong storm dataset with a target value of Eversource distribution system outages to be utilized as an additional input to the machine learning models. The strong storm data had 1178 storms, including but not limited to rain, wind and thunderstorm events, from Apr. 2005 to Mar. 2023 in its database. To find the storm index (i_{storm}), transmission lines were overlaid with distribution grid cells. For each transmission line, the total number of grid cells it intersected with was identified and the average prediction (p_{avg}) was taken. The average is then normalized by dividing it by the total number of assets (a_{tot}) in the grid cells (eq. 1).

$$\frac{p_{\text{avg}}}{a_{\text{tot}}} = i_{\text{storm}} \quad (1)$$

F. EVALUATION METRICS

The evaluation of machine learning models requires the use of appropriate metrics to assess their performance. Here, two metrics, mean absolute percentage error, and ranked predictions are used to understand model performance.

1) MEAN ABSOLUTE PERCENTAGE ERROR

Mean Absolute Percentage Error (MAPE) is a way to measure how accurate a prediction is. It is calculated by taking the difference between the predicted value and actual value, then dividing by the actual value and multiplying by 100. This method allows for understanding the total bias in the model predictions.

2) RANKED PREDICTIONS

The ranked predictions work by looking at 10 different percentiles of the predictions for all storms in database. For each percentile, the actual failures are counted to identify how

many failures the model was able to capture. For example, for the 14,124 data points, in the first decile or top 10% of transmission lines, which are ranked by highest failure risk, approximately the first 1,412 of ranked predictions are looked at to identify how many actual failures it was able to capture. Similarly, for the fifth decile, the top half of transmission lines, as ranked by failure risk, or approximately the first 7,062 of ranked predictions, are used to identify how many actual failures the model captures. This ranked method provides an understanding of which model is able to pick up on actual failure events faster than the others, by comparing how highly the actual transmission failures are ranked amongst the model outputs of failure risk for all transmission lines during storms.

III. RESULTS & DISCUSSION

Our first goal was to explore ways to reduce the bias in predictions from the initial FPM prototype, as the sum of failure risk predictions significantly exceeded the actual number of failures by an order of magnitude. Several approaches were considered to address this issue, but the key factor leading to the most significant improvement was the removal of the penalization component. In the previous model, the scikit-learn “balanced” class weighting was used, which automatically adjusts the weight of each sample inversely proportional to the class frequency in the input data. Since failures were rare in the dataset, this weighting heavily influenced the model during training. As a result, the model became biased, overemphasizing the minority class of failures.

In machine learning, when a model makes an incorrect prediction—i.e., when its output significantly deviates from the actual value—the loss function assigns a high value to that prediction error. This signals to the model that its predictions were off, prompting it to adjust its parameters in the next iteration. The larger the error, the greater the correction applied during training, allowing the model to focus more on areas where it performed poorly. However, the use of excessive penalties for incorrect predictions can skew this

learning process. By removing the penalization component, the model was able to learn in a more balanced manner, adjusting its parameters based on the true relationships in the data rather than disproportionately emphasizing rare errors. This change allowed the model to treat the dataset more naturally, leading to better performance and more accurate predictions.

Three techniques were used to interpret the model outputs: (i) summing the total predictions, (ii) ranking the predictions and examining percentiles, and (iii) observing the spatial distribution of the predictions. Summing the total predictions provides insights into the model's bias and variance. Ranking the predictions in descending order and analyzing the percentiles helps assess overall model performance, the speed at which the model captures predictions, and highlights important misclassifications.

TABLE 1. Model performance.

	Actual	Model 1 Previous	Model 2 Current	Model 3 Integrated	Model 4 Storm Index
# of failures	111	3832.29	94.97	93.87	93.67
MAPE	—	3352%	14.46%	15.43%	15.42%

Table 1 displays the actual number of failures, summed predictions of failures, and the bias for each model. Model 1 is the first prototype of FPM, which is the previous model used in [65]. Model 2 is the second prototype of the FPM, developed in this study through variable selection, hyperparameter tuning, and cross-validation. Model 3 is the third prototype of the FPM, an integrated model developed in this study, which incorporates fragility curve numbers as an additional input to the machine learning model. Model 4 is the fourth prototype of the FPM, known as the storm index model, which uses damage data from the distribution system to provide the machine learning model with information about various storms.

Models 2, 3, and 4 were able to reduce model bias by approximately two orders of magnitude compared to Model

1. Although the outputs of Models 2, 3, and 4 sum to 94.97, 93.87, and 93.67, respectively, and are much closer to the total actual failures of 111, Model 2 (14.46%) has a lower mean absolute percentage error than Model 3 (15.43%) and Model 4 (15.42%).

In our analytical approach, we explore a spatial perspective to gain insights into the viability of the models. By examining the spatial distribution of the data, we aimed to identify performance patterns across different regions. Specifically, we assessed the average predictions for each transmission line across all 44 storms, comparing these against the actual average failure data. This comparative analysis helped pinpoint areas where the models tended to over-predict or under-predict failures. Transmission lines were color-coded based on the values of their mean actual and predicted failures. The colormap ranged from 0 to 0.06, representing the range of mean actual failures. Dark red represented values of 0.06 or above (Figure 5).

The average actual failures range from 0.02 to 0.05 in the southeast of New Hampshire. In Western Massachusetts, the average failure value for transmission lines in the northwest of the state is 0.06, with connecting lines showing lower values between 0.025 and 0.04. In Connecticut, there is a pattern of decreasing average failure values as you move further inland from the coast. Along the coastline, values range from 0.045 to 0.06. Further inland, values range from 0.025 to 0.045. At the Connecticut-Massachusetts border, values range from 0.025 to 0.028. These values are understandable because, near the coast, the cyclical difference between sea and land breezes creates gusty winds, contributing to transmission failures.

Model 1 consistently predicts average failures of 0.06 or higher for all transmission lines. This model tends to over-predict failures, making it less effective in accurately assessing transmission line risk.

The results of Models 2, 3, and 4 align more closely with actual average failure occurrences, demonstrating greater variability in model predictions compared to Model 1, with slight differences observed between the three models.

The average predicted failures for Models 2, 3, and 4 are approximately 0.01 in the southeast of New Hampshire. For other lines in the state, the predicted values were below 0.005. In Western Massachusetts, the average value for transmission lines in the northwest of the state ranges from 0.038 to 0.042, with connecting lines showing lower values between 0.005 and 0.015. In Connecticut, the same pattern of decreasing average failure values with increasing distance from the coastline, observed in the actual failure data, is also seen in the results from these three models. Along the coastline, values range from 0.015 to 0.06. Further inland, toward the border of Connecticut and Massachusetts, the values range from 0.005 to 0.018.

We examine the ranking of these predictions to assess model improvements. Figure 6 shows the four models and their ranked predictions for each percentile. Each percentile is represented by a different color, and markers indicate the

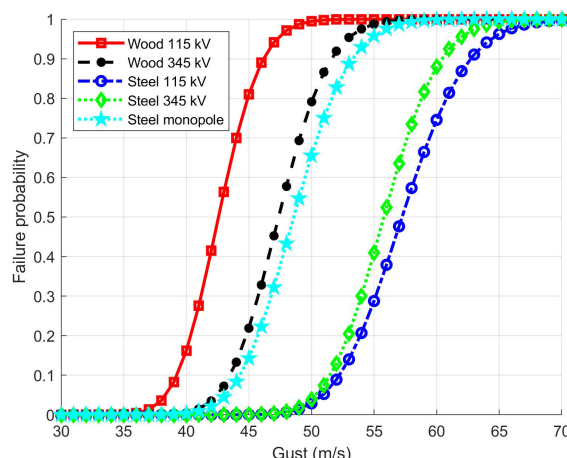


FIGURE 4. Sample fragility curves for different structure types from [66].

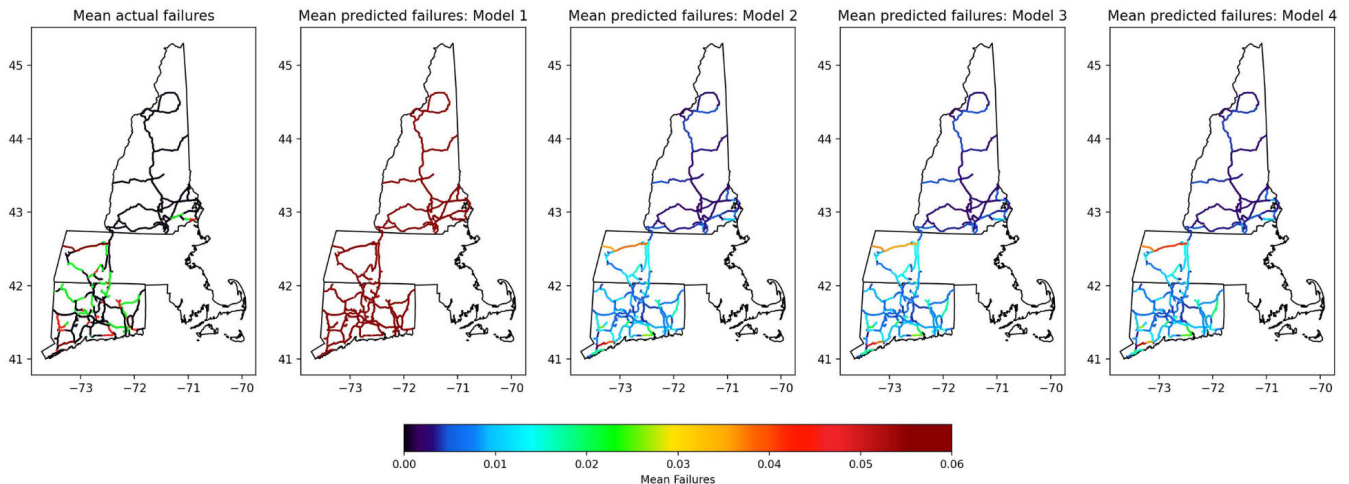


FIGURE 5. Spatial plot showing the mean average of actual and predicted failures, with a colormap ranging from black/purple (representing the lowest values) to red (representing the highest values), highlighting the variation in mean failure intensity across the regions.

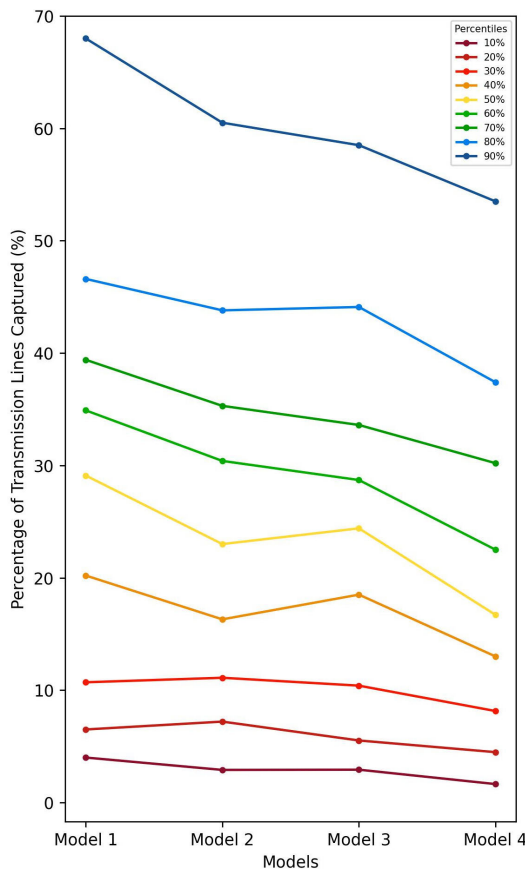


FIGURE 6. Plot of all model performances using ranked predictions, where different colored lines represent distinct percentiles.

model's performance for each percentile. Model 1 serves as the baseline to understand the improvements demonstrated by the three new models introduced in this study. Additional components added to Model 2 to create Models 3 and 4 were designed to provide marginal improvements, particularly in ranking lines with failures as having higher risk compared

to others in the transmission network, based on the ranked predictions metric.

This figure shows that 10% of total failures from the storms are captured within the top 4.00%, 2.90%, 2.92%, and 1.64% of ranked transmission line failure risk predictions for Models 1, 2, 3, and 4, respectively. To capture 60% of total failures from the storms, Models 1, 2, 3, and 4 capture the identified risk within the top 34.9%, 30.4%, 28.7%, and 22.5% of ranked transmission line failure risk predictions, respectively. For 90% of total failures, Models 1, 2, 3, and 4 identify the risk within the top 68.0%, 60.5%, 58.5%, and 53.5% of ranked risk predictions, respectively.

In capturing up to 20% of actual failures (between 0 and 20%), the models show relatively low variance in performance. After 20% of actual failures, the differences between the models begin to increase. The largest difference is seen between Models 1 and 4, particularly in the model's ability to capture failures between 50-60% of actual failures. Model 4 captures 50% of failures incurred during storms within approximately the top 20% of transmission lines ranked by modeled failure risk, whereas Model 1 captures 50% of failures within approximately the top 30% of transmission lines ranked by modeled failure risk. Across all models, Model 4 consistently demonstrates the ability to rank transmission lines with failures as highly as possible.

Model 2 captures failures faster between the 30th and 90th percentiles compared to Model 1. Model 3 captures failures faster only in the first three percentiles compared to Models 1 and 2. Model 4 captures failures the fastest across all percentiles among the models, likely due to the addition of distribution predictions, which improve the model's ability to learn from storm patterns and their impact on the transmission network.

Although Model 4 performs best, partly due to the addition of the storm index, it does not achieve better results due to the largely unbalanced historical transmission failure data.

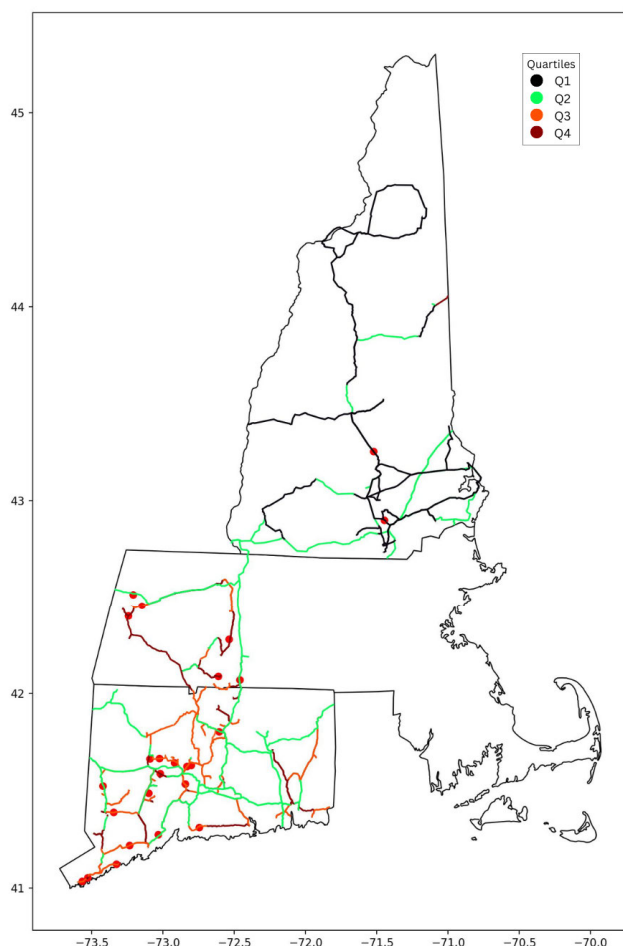


FIGURE 7. Spatial plot of model performance using ranked predictions for storm Isaias, where the red dots represent actual failure events and the different colored lines correspond to the four performance quartiles.

IV. CASE STUDY: STORM ISAIAS

This section presents a detailed analysis of Hurricane Isaias, illustrating the application and outcomes of the best-performing model discussed earlier. Hurricane Isaias made landfall near Ocean Isle Beach, North Carolina, on August 3 as a Category 1 storm. It weakened into a tropical storm as it moved north-northeastward inland along the Eastern Seaboard, reaching Albany, New York, on August 4 [88]. In this study, Isaias was the only storm that caused 25 transmission failures, while the next two storms in the dataset caused 9 and 5 failures, respectively. Model 4's predictions of transmission line failure risk for Isaias are displayed in quartiles, dividing the dataset into four parts (Figure 7). The color scheme is as follows: black for values at or below the first quartile (the lowest predicted failure risk), lime green for values between the first and second quartiles, orange for values between the second and third quartiles, and dark red for values between the third and fourth quartiles (the highest predicted failure risks).

In New Hampshire, the model showed minimal storm impacts in areas with failures, as all predictions fell within

the two lower quartiles. Despite limited historical data and relatively low storm activity in New Hampshire overall, the model identified areas of concern in the southern part of the state, where failures were observed. In Western Massachusetts, the model captured 5 of the 6 failures within the top 50% of transmission line failure risk predictions (the upper two quartiles). Additionally, 3 of those 5 failures occurred on transmission lines within the highest quartile. In Connecticut, where most of the failures occurred, the model was able to capture 14 of the 17 failures within the upper quartiles. The model also highlighted the central and coastal parts of the state, where the observed failures took place.

Utilizing this model before the storm Isaias would have been crucial for implementing preventive measures to minimize power failures. It could also have helped estimate the necessary number of crew members required to restore power in areas identified by the model. This proactive strategy could significantly improve preparedness and response efforts for future storms. By leveraging real-time data and predictive analytics, authorities can prioritize resources more efficiently and coordinate response efforts, potentially reducing the impact of severe weather on local communities.

V. CONCLUSION

This study presents a model capable of understanding and quantifying the impact of severe weather events on electric transmission systems. While distribution system weather impact models have seen substantial development, transmission system models have lagged due to limited data availability. This research addresses this gap by advancing a weather impact model focused on predicting transmission line failure probabilities. By refining techniques to reduce modeling bias through variable selection, hyper-parameter tuning, and integrating multiple modeling approaches, substantial improvements in accuracy were made. The usage of the integrated approaches, enhanced the model's ability to predict transmission risk, further reducing in model bias from 3352% to 14.46–15.43%, highlighting the capabilities of this integrated approach. Moreover, the model shows improved capabilities in identifying at-risk transmission lines, with the refined model capturing 60% of failures within the top 22.5% of ranked power lines, compared to just 34.9% for the previous model.

While this study provides valuable insights, it is important to acknowledge its limitations. The dataset is heavily imbalanced, with only around 1% of the data samples associated with failures—the target variable the model aims to predict. Future research would benefit from using a larger dataset with more failure occurrences for several reasons. First, it would help create a more robust model, as more data from storms with varying weather conditions would allow the model to learn from a broader range of scenarios, potentially improving its generalizability. Second, it is widely accepted in machine learning that more data samples lead to more accurate models, thereby boosting confidence in model

predictions. With more data, the model is also more likely to establish accurate relationships between inputs and the dependent variable (failures), resulting in better insights into feature importance and the relationships between features.

Future work includes computing transmission resilience, conducting climate studies, and analyzing total system risk. For transmission resilience, this model could be used to analyze key factors such as load capacity, redundancy, recovery time, and historical failure data, helping identify vulnerabilities within the transmission infrastructure. Additionally, it can simulate various scenarios to evaluate the system's response to extreme weather events, supporting the design of more robust systems to enhance overall resilience. For climate studies, the model presented in this work can be used alongside future climate projections to analyze how shifting climate conditions might impact transmission system resilience. This approach allows for the assessment of how various factors could affect existing infrastructure, offering valuable insights to inform planning for resilience improvements. By quantifying risks associated with different parts of the transmission system, an approach that pairs the model with climate scenarios can provide a comprehensive

TABLE 2. Final variable list used for model training.

Short name	Description	Source	Type
max_MeanWSpd10	Spatial maximum of the temporal mean of wind speed about 10 m/s	WRF	Weather
max_MeanGust	Spatial maximum of the temporal mean of wind gust	WRF	Weather
max_MaxTotPrec	Spatial maximum of the temporal maximum of total precipitation	WRF	Weather
max_MaxPrecRt	Spatial maximum of the temporal maximum of precipitation rate	WRF	Weather
max_MeanPrecRt	Spatial maximum of the temporal mean of precipitation rate	WRF	Weather
max_MeanSoilIM	Spatial maximum of the temporal mean of soil moisture	WRF	Weather
mean_MaxTemp	Spatial mean of the temporal max of temperature	WRF	Weather
max_MaxCAPE	Spatial maximum of the temporal max of convective available potential energy	WRF	Weather
max_MaxCIN	Spatial maximum of the temporal max of convective inhibition	WRF	Weather
43	Mixed Forest	NCLD	Vegetation
52	Shrub	NCLD	Vegetation
LC_Wetland	Summation of categories 11 (Open Water), 90 (Woody Wetlands), and 95 (Emergent Herbaceous Wet-lands)	NCLD	Vegetation
LC_No/LowVeg	Summation of categories 31 (Barren Land), 71 (Grassland/Herbaceous), 81 (Pasture/Hay), and 82 (Cultivated Crops)	NCLD	Vegetation
LAI	Leaf Area Index	MODIS	Vegetation
elev_mean	Mean elevation	ASTGTM	Topography
YearMin	Year at which the transmission poles were built	ISO-NE	Infrastructure
TotLen	Total length of each transmission line	ISO-NE	Infrastructure
StrCount	Number of transmission poles connected to each transmission line	ISO-NE	Infrastructure
Other%	Percentage of unidentified transmission pole type	ISO-NE	Infrastructure

view of the vulnerabilities affecting energy distribution. Further analysis of these vulnerabilities can help improve failure mitigation plans.

By providing advanced estimates of transmission line failure probabilities ahead of severe weather events, our findings empower power system planners and maintenance engineers to implement proactive mitigation strategies, minimizing disruptions and optimizing resilience investments. This research not only advances predictive modeling for transmission system resilience but also provides actionable insights essential for protecting transmission infrastructure during severe weather events.

APPENDIX

See Table 2.

REFERENCES

- [1] S. Guikema, R. Davidson, and H. Liu, "Statistical models of the effects of tree trimming on power system outages," *IEEE Trans. Power Del.*, vol. 21, no. 3, pp. 1549–1557, Jul. 2006.
- [2] M. Panteli and P. Mancarella, "Influence of extreme weather and climate change on the resilience of power systems: Impacts and possible mitigation strategies," *Electr. Power Syst. Res.*, vol. 127, pp. 259–270, Oct. 2015.
- [3] M. Panteli, P. Mancarella, D. N. Trakas, E. Kyriakides, and N. D. Hatziargyriou, "Metrics and quantification of operational and infrastructure resilience in power systems," *IEEE Trans. Power Syst.*, vol. 32, no. 6, pp. 4732–4742, Nov. 2017.
- [4] M. Panteli and P. Mancarella, "Modeling and evaluating the resilience of critical electrical power infrastructure to extreme weather events," *IEEE Syst. J.*, vol. 11, no. 3, pp. 1733–1742, Sep. 2017.
- [5] M. Panteli, C. Pickering, S. Wilkinson, R. Dawson, and P. Mancarella, "Power system resilience to extreme weather: Fragility modeling, probabilistic impact assessment, and adaptation measures," *IEEE Trans. Power Syst.*, vol. 32, no. 5, pp. 3747–3757, Sep. 2017.
- [6] N. Bhusal, M. Abdelmalak, M. Kamruzzaman, and M. Benidris, "Power system resilience: Current practices, challenges, and future directions," *IEEE Access*, vol. 8, pp. 18064–18086, 2020.
- [7] A. T. D. Perera, V. M. Nik, D. Chen, J.-L. Scartezzini, and T. Hong, "Quantifying the impacts of climate change and extreme climate events on energy systems," *Nature Energy*, vol. 5, no. 2, pp. 150–159, Feb. 2020.
- [8] A. E. Schweikert and M. R. Deinert, "Vulnerability and resilience of power systems infrastructure to natural hazards and climate change," *WIREs Climate Change*, vol. 12, no. 5, p. 724, Sep. 2021.
- [9] L. Dumarevskaya and J. R. Parent, "Electric grid resilience: The effects of conductor coverings, enhanced tree trimming, and line characteristics on tree-related power outages," *Electr. Power Syst. Res.*, vol. 221, Aug. 2023, Art. no. 109454.
- [10] J. M. Boggess, G. W. Becker, and M. K. Mitchell, "Storm & flood hardening of electrical substations," in *Proc. IEEE PES T&D Conf. Expo.*, Chicago, IL, USA, Apr. 2014, pp. 1–5.
- [11] *New England Power Grid 2022-2023 Profile*, ISO-NE, Holyoke, MA, USA, Feb. 2023.
- [12] R. Aggarwal, A. Johns, J. Jayasinghe, and W. Su, "An overview of the condition monitoring of overhead lines," *Electr. Power Syst. Res.*, vol. 53, pp. 15–22, Jan. 2000.
- [13] J. Beyza and J. M. Yusta, "The effects of the high penetration of renewable energies on the reliability and vulnerability of interconnected electric power systems," *Rel. Eng. Syst. Saf.*, vol. 215, Nov. 2021, Art. no. 107881.
- [14] S. Das and Z. Wang, "Power grid vulnerability analysis with rising renewables infiltration," *J. Syst., Cybern. Informat.*, vol. 19, pp. 23–32, Jul. 2021.
- [15] G. Sarma and A. Zabanioti, "Understanding vulnerabilities of renewable energy systems for building their resilience to climate change hazards: Key concepts and assessment approaches," *Renew. Energy Environ. Sustainability*, vol. 6, p. 35, Oct. 2021.
- [16] S. K. Kim and S. Park, "Impacts of renewable energy on climate vulnerability: A global perspective for energy transition in a climate adaptation framework," *Sci. Total Environ.*, vol. 859, Feb. 2023, Art. no. 160175.

- [17] L. Hartman, "Wind turbine in extreme weather: Solutions for hurricane resiliency," Office Energy Efficiency Renew. Energy, Jan. 2018. [Online]. Available: <https://www.energy.gov/eere/articles/wind-turbines-extreme-weather-solutions-hurricane-resiliency>
- [18] *Transmission Line Vegetation Management*, Federal Energy Regulation Commission, Washington, DC, USA, Nov. 2023.
- [19] R. Thorson, "The power grid's Achilles' squirrels," Dept. of Earth Sciences, Univ. Connecticut, Storrs, CT, USA, 2021. [Online]. Available: <https://earthsciences.uconn.edu/2021/07/19/the-power-grids-achilles-squirrels/>
- [20] H. Long, L. Wang, Z. Zhang, Z. Song, and J. Xu, "Data-driven wind turbine power generation performance monitoring," *IEEE Trans. Ind. Electron.*, vol. 62, no. 10, pp. 6627–6635, Oct. 2015.
- [21] H. Sharma, L. Marinovici, V. Adetola, and H. T. Schaeff, "Data-driven modeling of power generation for a coal power plant under cycling," *Energy AI*, vol. 11, Jan. 2023, Art. no. 100214.
- [22] S. Al-Dahidi, M. Madhiarasan, L. Al-Ghussain, A. M. Abubaker, A. D. Ahmad, M. Alrbai, M. Aghaei, H. Alahmer, A. Alahmer, P. Baraldi, and E. Zio, "Forecasting solar photovoltaic power production: A comprehensive review and innovative data-driven modeling framework," *Energies*, vol. 17, no. 16, p. 4145, 2024.
- [23] N. Mohan, K. P. Soman, and S. S. Kumar, "A data-driven strategy for short-term electric load forecasting using dynamic mode decomposition model," *Appl. Energy*, vol. 232, pp. 229–244, Dec. 2018.
- [24] K. D. Ünlü, "A data-driven model to forecast multi-step ahead time series of Turkish daily electricity load," *Electronics*, vol. 11, p. 1524, May 2022.
- [25] S. Mukherjee and R. Nateghi, "A data-driven approach to assessing supply inadequacy risks due to climate-induced shifts in electricity demand," *Risk Anal.*, vol. 39, no. 3, pp. 673–694, Mar. 2019.
- [26] C. Ning and F. You, "Data-driven adaptive robust unit commitment under wind power uncertainty: A Bayesian nonparametric approach," *IEEE Trans. Power Syst.*, vol. 34, no. 3, pp. 2409–2418, May 2019.
- [27] J. He, Z. Lv, and X. Chen, "Rolling bearing fault diagnosis method based on 2D grayscale images and Wasserstein generative adversarial nets under unbalanced sample condition," *Complex Eng. Syst.*, vol. 3, pp. 1–15, Aug. 2023.
- [28] B. Basciftci, S. Ahmed, and N. Gebraeel, "Data-driven maintenance and operations scheduling in power systems under decision-dependent uncertainty," *IIE Trans.*, vol. 52, no. 6, pp. 589–602, Jun. 2020.
- [29] H. Gilani, H. Sahebi, and M. S. Pishvaee, "A data-driven robust optimization model for integrated network design solar photovoltaic to micro grid," *Sustain. Energy, Grids Netw.*, vol. 31, Sep. 2022, Art. no. 100714.
- [30] M. Shen, X. Wang, S. Zhu, Z. Wu, and T. Huang, "Data-driven event-triggered adaptive dynamic programming control for nonlinear systems with input saturation," *IEEE Trans. Cybern.*, vol. 54, no. 2, pp. 1178–1188, Feb. 2024.
- [31] T. M. Alabi, E. I. Aghimien, F. D. Agbajor, Z. Yang, L. Lu, A. R. Adeoye, and B. Gopaluni, "A review on the integrated optimization techniques and machine learning approaches for modeling, prediction, and decision making on integrated energy systems," *Renew. Energy*, vol. 194, pp. 822–849, Jul. 2022.
- [32] A. F. Mensah and L. Duenas-Osorio, "Outage predictions of electric power systems under hurricane winds by Bayesian networks," in *Proc. Int. Conf. Probabilistic Methods Appl. Power Syst. (PMAPS)*, Durham, U.K., Jul. 2014, pp. 1–6.
- [33] D. W. Wanik, E. N. Anagnostou, B. M. Hartman, M. E. B. Frediani, and M. Astitha, "Storm outage modeling for an electric distribution network in northeastern USA," *Natural Hazards*, vol. 79, no. 2, pp. 1359–1384, Nov. 2015.
- [34] J. He, D. W. Wanik, B. M. Hartman, E. N. Anagnostou, M. Astitha, and M. E. B. Frediani, "Nonparametric tree-based predictive modeling of storm outages on an electric distribution network," *Risk Anal.*, vol. 37, no. 3, pp. 441–458, Mar. 2017.
- [35] B. A. Alpay, D. Wanik, P. Watson, , G. Liang, and E. Anagnostou, "Dynamic modeling of power outages caused by thunderstorms," *Forecasting*, vol. 2, no. 2, pp. 151–162, May 2020.
- [36] , , P. Watson, and E. N. Anagnostou, "Outage prediction models for snow and ice storms," *Sustain. Energy, Grids Netw.*, vol. 21, Mar. 2020, Art. no. 100294.
- [37] Y. Kor, M. Z. Reformat, and P. Musilek, "Predicting weather-related power outages in distribution grid," in *Proc. IEEE Power Energy Soc. Gen. Meeting (PESGM)*, Montreal, QC, Canada, Aug. 2020, pp. 1–5.
- [38] B. Li, Y. Chen, S. Huang, H. Guan, Y. Xiong, and S. Mei, "A Bayesian network model for predicting outages of distribution system caused by hurricanes," in *Proc. IEEE Power Energy Soc. Gen. Meeting (PESGM)*, Montreal, QC, Canada, Aug. 2020, pp. 1–5.
- [39] F. Yang, P. Watson, , and E. N. Anagnostou, "Enhancing weather-related power outage prediction by event severity classification," *IEEE Access*, vol. 8, pp. 60029–60042, 2020.
- [40] Y. Du, Y. Liu, X. Wang, J. Fang, G. Sheng, and X. Jiang, "Predicting weather-related failure risk in distribution systems using Bayesian neural network," *IEEE Trans. Smart Grid*, vol. 12, no. 1, pp. 350–360, Jan. 2021.
- [41] R. Tervo, I. Lång, A. Jung, and A. Mäkelä, "Predicting power outages caused by extratropical storms," *Natural Hazards Earth Syst. Sci.*, vol. 21, pp. 607–627, Feb. 2021.
- [42] O. S. Omogoye, K. A. Folly, and K. O. Awodele, "Enhancing the distribution power system resilience against hurricane events using a Bayesian network line outage prediction model," *J. Eng.*, vol. 2021, no. 11, pp. 731–744, Nov. 2021.
- [43] F. Yang, , and E. N. Anagnostou, "The effect of lead-time weather forecast uncertainty on outage prediction modeling," *Forecasting*, vol. 3, no. 3, pp. 501–516, Jul. 2021.
- [44] , W. Zhang, , A. Bagtzoglou, D. Wanik, and E. Anagnostou, "A hybrid physics-based and data-driven model for power distribution system infrastructure hardening and outage simulation," *Rel. Eng. Syst. Saf.*, vol. 225, Sep. 2022, Art. no. 108628.
- [45] F. G. Hirata, "Mapping and modelling the probability of tree-related power outages using topographic, climate, and stand data," M.S. thesis, Fac. Graduate Stud., Univ. Brit. Columbia, Vancouver, BC, USA, 2011.
- [46] M. Doostan, R. Sohrabi, and B. Chowdhury, "A data-driven approach for predicting vegetation-related outages in power distribution systems," *Int. Trans. Electr. Energy Syst.*, vol. 30, Jan. 2020, Art. no. e12154.
- [47] P. L. Watson, , and E. N. Anagnostou, "Dynamic modeling of the effects of vegetation management on weather-related power outages," *Electric Power Syst. Res.*, vol. 207, Jun. 2022, Art. no. 107840.
- [48] , D. Wanik, , and E. N. Anagnostou, "Community power outage prediction modeling for the eastern United States," *Energy Rep.*, vol. 10, pp. 4148–4169, Nov. 2023.
- [49] Y. Du, Y. Liu, Y. Yan, J. Fang, and X. Jiang, "Risk management of weather-related failures in distribution systems based on interpretable extra-trees," *J. Modern Power Syst. Clean Energy*, vol. 11, no. 4, pp. 1868–1877, 2023.
- [50] A. Arif and Z. Wang, "Distribution network outage data analysis and repair time prediction using deep learning," in *Proc. IEEE Int. Conf. Probabilistic Methods Appl. Power Syst. (PMAPS)*, Jun. 2018, pp. 1–6.
- [51] H. Li, L. A. Treinish, and J. R. M. Hosking, "A statistical model for risk management of electric outage forecasts," *IBM J. Res. Develop.*, vol. 54, no. 3, pp. 8:1–8:11, May 2010.
- [52] W. Zhang, W. Sheng, K. Liu, S. Du, D. Jia, and L. Hu, "Fault prediction method for distribution network outage based on feature selection and ensemble learning," in *Proc. 5th Int. Conf. Inf. Sci. Control Eng. (ICISCE)*, Zhengzhou, China, Jul. 2018, pp. 226–231.
- [53] S. Das, P. Kankanala, and A. Pahwa, "Outage estimation in electric power distribution systems using a neural network ensemble," *Energies*, vol. 14, no. 16, p. 4797, Aug. 2021.
- [54] F. S. Kebede, J.-C. Olivier, S. Bourguet, and M. Machmoum, "Reliability evaluation of renewable power systems through distribution network power outage modelling," *Energies*, vol. 14, no. 11, p. 3225, May 2021.
- [55] J. Huang, C. Chen, C. Sun, Y. Cao, and Y. An, "An integrated risk assessment model for the multi-perspective vulnerability of distribution networks under multi-source heterogeneous data distributions," *Int. J. Electr. Power Energy Syst.*, vol. 153, Nov. 2023, Art. no. 109397.
- [56] B. Shen, D. Koval, and S. Shen, "Modelling extreme-weather-related transmission line outages," in *Proc. Eng. Solutions Next Millennium. IEEE Can. Conf. Electr. Comput. Eng.*, vol. 3, May 1999, pp. 1271–1276.
- [57] S. Guikema and S. Quiring, "Hybrid data mining-regression for infrastructure risk assessment based on zero-inflated data," *Rel. Eng. Syst. Saf.*, vol. 99, pp. 178–182, Mar. 2012.
- [58] S. Hartling, V. Sagan, M. Maimaitijiang, W. Dannevik, and R. Pasken, "Estimating tree-related power outages for regional utility network using airborne LiDAR data and spatial statistics," *Int. J. Appl. Earth Observ. Geoinf.*, vol. 100, Aug. 2021, Art. no. 102330.

- [59] M. Papic, D. Angell, P. Van Patten, and B. Efaw, "Historical performance analysis of transmission lines using Idaho power company's outage database GTORS," in *Proc. IEEE Int. Conf. Probabilistic Methods Appl. Power Syst. (PMAPS)*, Jun. 2018, pp. 1–6.
- [60] G. Fu, S. Wilkinson, R. J. Dawson, H. J. Fowler, C. Kilsby, M. Panteli, and P. Mancarella, "Integrated approach to assess the resilience of future electricity infrastructure networks to climate hazards," *IEEE Syst. J.*, vol. 12, no. 4, pp. 3169–3180, Dec. 2018.
- [61] T. Dokic, M. Pavlovski, D. Gligorijevic, M. Kezunovic, and Z. Obradovic, "Spatially aware ensemble-based learning to predict weather-related outages in transmission," in *Proc. Hawaii Int. Conf. Syst. Sci. (HICSS)*, Jan. 2019, pp. 1–10.
- [62] Y. Xie, C. Li, Y. Lv, and C. Yu, "Predicting lightning outages of transmission lines using generalized regression neural network," *Appl. Soft Comput.*, vol. 78, pp. 438–446, May 2019.
- [63] T. Alquthami, M. K. Alghamdi, B. S. Almajnuni, and O. M. Alarbidi, "Forecasting transmission system outages using artificial neural networks," in *Proc. 22nd Int. Middle East Power Syst. Conf. (MEPCON)*, Assiut, Egypt, Dec. 2021, pp. 654–658.
- [64] F. M. Shakiba, M. Shojaee, S. M. Azizi, and M. Zhou, "Real-time sensing and fault diagnosis for transmission lines," *Int. J. Netw. Dyn. Intell.*, vol. 1, pp. 36–47, Dec. 2022.
- [65] , , , , , F. Yang, , , and E. N. Anagnostou, "Machine learning evaluation of storm-related transmission outage factors and risk," *Sustain. Energy, Grids Netw.*, vol. 34, Jun. 2023, Art. no. 101016.
- [66] , , , , M. Hong, X. Luo, , , E. Anagnostou, and W. Zhang, "A probabilistic method for integrating physics-based and data-driven storm outage prediction models for power systems," *ASCE-ASME J. Risk Uncertainty Eng. Syst., A, Civil Eng.*, vol. 10, no. 2, Jun. 2024, Art. no. 04024021.
- [67] , , D. W. Wanik, M. A. E. Bhuiyan, X. Zhang, J. Yang, M. E. B. Frediani, and E. N. Anagnostou, "Predicting storm outages through new representations of weather and vegetation," *IEEE Access*, vol. 7, pp. 29639–29654, 2019.
- [68] W. C. Skamarock, "A description of the advanced research WRF version 3," NCAR, Boulder, CO, USA, Tech. Rep. NCAR/TN475+STR, 2008.
- [69] W. Wang, C. Bruyère, M. Duda, J. Dudhia, D. Gill, and H.-C. Lin, "ARW version 3 modelling system user's guide," Mesoscale Microscale Meteorol., Nat. Center Atmos. Res., Tech. Rep. 312, 2010.
- [70] J. Dewitz, "National land cover database (NLCD) 2021 products," Tech. Rep., 2023.
- [71] U. S. F. Service, "Individual tree species parameter maps," Tech. Rep., 2015.
- [72] P. Potapov, X. Li, A. Hernandez-Serna, A. Tyukavina, M. C. Hansen, A. Kommareddy, A. Pickens, S. Turubanova, H. Tang, C. E. Silva, J. Armstrong, R. Dubayah, J. B. Blair, and M. Hofton, "Mapping global forest canopy height through integration of GEDI and Landsat data," *Remote Sens. Environ.*, vol. 253, Feb. 2021, Art. no. 112165.
- [73] *Leaf Area Index (1 Month Terra/MODIS)*, NASA Earth Observations (NEO), Washington, DC, USA, 2017.
- [74] *ASTER Global Digital Elevation Model V003*, NASA/METI/AIST/Japan Spacesystems U.S./Japan ASTER Sci. Team, Washington, DC, USA, 2019.
- [75] A. U. Melagoda, T. D. L. P. Karunaratna, G. Nisaharan, P. A. G. M. Amarasinghe, and S. K. Abeygunawardane, "Application of machine learning algorithms for predicting vegetation related outages in power distribution systems," in *Proc. 3rd Int. Conf. Electr. Eng. (EECon)*, Sep. 2021, pp. 25–30.
- [76] N. Cristianini and E. Ricci, "Support vector machines: 1992; Boser, Guyon, Vapnik," in *Encyclopedia of Algorithms*, M.-Y. Kao, Ed., Boston, MA, USA: Springer, 2008, pp. 928–932.
- [77] A. Mucherino, P. J. Papajorgji, and P. M. Pardalos, "k-nearest neighbor classification," in *Data Mining in Agriculture* (Springer Optimization and Its Applications), vol. 34. New York, NY, USA: Springer, 2009, pp. 83–106.
- [78] L. Breiman, "Random forests," *Mach. Learn.*, vol. 45, no. 1, pp. 5–32, 2001.
- [79] J. H. Friedman, "Greedy function approximation: A gradient boosting machine," *Ann. Statist.*, vol. 29, no. 5, pp. 1189–1232, Oct. 2001.
- [80] T. Chen and C. Guestrin, "XGBoost: A scalable tree boosting system," in *Proc. 22nd ACM SIGKDD Int. Conf. Knowl. Discovery Data Mining*, San Francisco, CA, USA, Aug. 2016, pp. 785–794.
- [81] D. M. Allen, "The relationship between variable selection and data augmentation and a method for prediction," *Technometrics*, vol. 16, no. 1, pp. 125–127, Feb. 1974.
- [82] M. Stone, "Cross-validatory choice and assessment of statistical predictions," *J. Roy. Stat. Soc. Ser. B, Stat. Methodol.*, vol. 36, no. 2, pp. 111–133, Jan. 1974.
- [83] S. Geisser, "The predictive sample reuse method with applications," *J. Amer. Stat. Assoc.*, vol. 70, pp. 320–328, Jun. 1975.
- [84] S. Kotsiantis, "Feature selection for machine learning classification problems: A recent overview," *Artif. Intell. Rev.*, vol. 42, no. 1, pp. 157–176, 2011.
- [85] L. Yang and A. Shami, "On hyperparameter optimization of machine learning algorithms: Theory and practice," *Neurocomputing*, vol. 415, pp. 295–316, Nov. 2020.
- [86] T. Yu and H. Zhu, "Hyper-parameter optimization: A review of algorithms and applications," 2020, *arXiv:2003.05689*.
- [87] S. M. LaValle, M. S. Branicky, and S. R. Lindemann, "On the relationship between classical grid search and probabilistic roadmaps," *Int. J. Robot. Res.*, vol. 23, pp. 673–692, Aug. 2004.
- [88] *Summary of Tropical Storm Isaias*, Nat. Weather Service, Silver Spring, MD, USA, Oct. 2020.



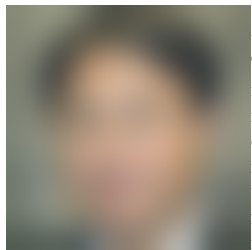
(Member, IEEE) received the B.A. degree in anthropology and the B.S.E. degree in environmental engineering from the University of Connecticut, Storrs, CT, USA, in 2018 and 2021 respectively, where she is currently pursuing the Ph.D. degree in environmental engineering with the Department of Civil and Environmental Engineering. Her primary Ph.D. research focuses on weather impact modeling using applied meteorological process for natural and the built environment. Her other research interests include wildfire ignition modeling, electric grid reliability, and resiliency and storm impact mitigation.



received the B.S. degree in mechanical engineering, the M.S. degree in business analytics and project management, and the Ph.D. degree in environmental engineering from the University of Connecticut, Storrs, CT, USA, in 2014, 2019, and 2023, respectively. The work for this article was conducted during the Ph.D. degree. He is currently with the Electric Power Research Institute (EPRI), where his research focuses on many facets of distributed energy resource (DER) interconnection and electric grid resilience.



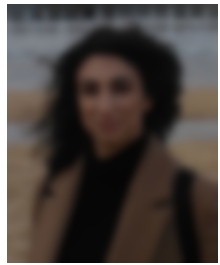
received the B.S.E. and Ph.D. degrees in civil engineering from the University of Connecticut, Storrs, CT, USA, in 2019 and 2023, respectively. The work for this article was conducted during the Ph.D. degree. He is currently a Postdoctoral Researcher with the Community Resilience Group, Engineering Laboratory, National Institute of Standards and Technology. His research interests include modeling the resilience of infrastructure systems to natural hazards, encompassing fragility assessment of structures under multi-hazards, integrating machine learning and physics-based models for improved hazard impact predictions, and optimization of retrofit and mitigation actions to reduce disaster impacts to communities.



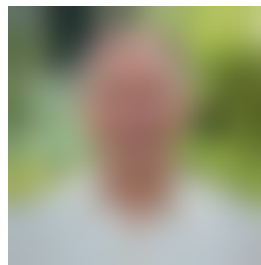
(Member, IEEE) received the B.E. degree in electrical engineering from Tsinghua University, in 1991, the M.S. degree in mathematics from the University of Minnesota, in 1993, and the Ph.D. degree in electrical engineering from the University of Washington, in 1998. He was a Power Systems Engineer with ALSTOM Grid, Redmond, WA, USA, from 1998 to 2005; an Associate Professor of mathematics with Valley Forge Military College, from 2005 to 2006; and a Principle Market Engineer with the Mid-Continent Independent System Operator, Carmel, IN, USA, from 2006 to 2012. He was an Associate Professor with the Electrical Engineering and Computer Science Department, Case Western Reserve University, Cleveland, OH, USA, from 2012 to 2018. He is currently a Principal Analyst with ISO New England Inc., Holyoke, MA, USA. His research interests include power system analysis, electricity markets, and smart distribution systems.



(Senior Member, IEEE) is currently the Manager of the Power System Technology Group, ISO New England Inc. He is responsible for the technology strategy, research, and development of bulk power system operations and planning. He has more than 80 academic publications. He received the 2021 Energy Central Innovation Champion Award. He is the Vice Chair of the IEEE PES Working Group “Cloud4PowerGrid,” IEEE Corporate Engagement liaison for ISO New England Inc., and the Past Chair of the IEEE PES Technologies and Innovation Subcommittee.



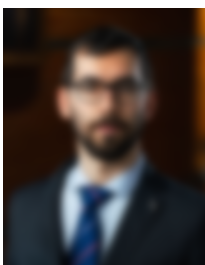
received the B.S. degree in geography from Harokopio University, Kallithea, Athens, Greece, in 2011, the M.Sc. degree in environmental physics and meteorology from the University of Athens, Athens, in 2015, and the Ph.D. degree in environmental engineering from the University of Connecticut, Storrs, CT, USA, in 2021. She is currently a Senior SNSF Researcher with the Institute of Earth Surface Dynamics (IDYST), University of Lausanne. Her research interests include developing a better understanding of the dynamics and predictability of hydro-meteorological extremes with a focus on the land surface-atmosphere interactions.



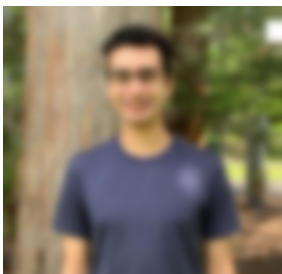
(Senior Member, IEEE) received the M.S., Ph.D., and Doctor of Sciences degrees in power systems from Peter the Great St.Petersburg Polytechnic University, in 1979, 1984, and 1998, respectively. He is currently the Technical Manager of the Advanced Technology Solutions Department, ISO New England Inc., with a focus on research and development in areas of power system resilience, operations, stability, cascading analysis, synchrophasors, and smart grids.



received the M.S. degree in environmental engineering from Dalian University of Technology, Ganjingzi, Dalian, Liaoning, China, and the M.S. degree in computer science and engineering and the Ph.D. degree in environmental engineering from the University of Connecticut, Storrs, CT, USA. She specializes in using machine learning for the prediction of electrical outages from severe and extreme weather events in distribution and transmission systems. Her research interests include but are not limited to, wildfire ignition prediction, electric grid vulnerability, and climate change analysis.



received the B.S. degree in physics from the University of Pisa, Italy, in 2012, the M.S. degree in physics of the Earth system from the University of Bologna, Italy, in 2015, and the Ph.D. degree in environmental engineering from the University of Connecticut, Storrs, CT, USA, in 2019. Since 2020, he has been an Assistant Professor with the Department of Civil and Environmental Engineering, University of Connecticut, and the Manager of the Eversource Energy Center. Since 2022, he has been the Associate Director of Storm Preparedness and Emergency Response with the Eversource Energy Center. His research interests include weather impact modeling for electric transmission and distribution networks, grid resilience analysis, and renewable energy integration. He is an Alumnus of the National Academy of Engineering (NAE) and the Grainger Foundation Frontiers of Engineering (FOE).



received the B.S.E. degree in electrical engineering, the B.S. degree in mathematics, and the M.S. degree in environmental engineering from the University of Connecticut, Storrs, CT, USA, in 2021, 2021, and 2023, respectively. He is currently pursuing the Ph.D. degree in environmental engineering with the Department of Civil and Environmental Engineering, Princeton University. His research interests include centered around the effects of extreme weather events. Recently, he has been recognized with a State of Connecticut General Assembly Citation for his significant contributions to the International Space Station.